Sparse Source Location for Real Aperture Radar Using Generalized SPICE Approach

Yongchao Zhang, Yin Zhang, Yulin Huang, Jianyu Yang
University of Electronic Science and Technology of China
Chengdu, Sichuan 611731
Email: zhang_yongchao1@163.com

Andreas Jakobsson
Lund University
SE-221 00 Lund, Sweden
Email: aj@maths.lth.se

***Abstract*—Source location for real aperture radar (RAR) has raised many concerns in the fields of ground-based monitoring for aircrafts and vessels. However, the resolution of RAR in azimuth is constrained by the antenna beam width, which results in low degree of location accuracy. In this paper, a superresolution methodology to locate sources is proposed by exploiting the inherent sparseness of the target distribution. Based on the weighted covariance fitting criterion, we first introduce the popular SParse Iterative Covariance-based Estimation (SPICE) approach to improve the angular resolution. Furthermore, to increase the sparseness and location accuracy, a varying penalty on noise term is adopted to extend the SPICE method generally. Numerical results validates that the generalized SPICE method enjoys improved resolution and higher locationthe accuracy when compared with the RAR system and existing superresolution algorithms.**

I. Introduction

Real aperture radar (RAR) is an old-line active microwave sensor which was originally developed for target detection, location and Doppler estimation. With the advantage of arbitrary imaging geometry, it plays a significant role in modern civil applications where synthetic aperture radar fails to work. For example, the RAR fixed on the ground can be applied to the airport (Airport Surveillance Radar) or harbour for real-time monitoring the aircrafts or vessels [1]. This can improve the safety of the flight or tracking the vessels in all-day and all-weather condition.

However, the cross-range resolution of RAR is constrained by the real aperture size D, carrier wavelength λ and directly proportional to the distance R [1]:

$$\delta_{cr} \approx \frac{R\lambda}{D} \tag{1}$$

Typically, if $\lambda = 2.5cm$ (X-band) and $D = 2m$, then the cross-range resolution at distance $R = 100km$ will be $\delta_{cr} \approx 1.25km$. The coarse resolution would lead a wrong location when there are multiple targets within the beamwidth. Theoretically, the azimuth resolution can be improved by operating at higher frequencies or increasing the aperture. But if exceptionally high frequencies are used, detection ranges are reduced by atmospheric attenuation, and there are practical limitations on the platform size.

To improve the azimuth resolution of RAR, the superresolution technique has received substantial and well-justified interest over the past decades. Because RAR works in scanning mode to cover the whole imaging area, superresolution can be interpreted as an ill-conditioned linear inversion problem with the scanning measurements. To deal with the ill-conditioned problem, several regularization methods have been proposed in the literature. In [2], a stable and effective approach based on Tikhonov regularization procedure (REGU) is proposed. In [3], the author proposes the truncated singular value decomposition (TSVD) method to improve the coarse resolution. In [4], [5], the different iterative schemes of the Landweber method that converge to the desired solution are presented. The REGU, TSVD, and Landweber approaches are shown to minimize the noise noticeably. However, this improvement comes at the cost of limited resolution enhancement.

To obtain higher resolution, the maximum a posteriori-based superresolution method was developed in [6]. It can provide higher azimuth resolution but suffers from a high estimation error and blurring effect for low SNR. In [7], [8], [9], [10], [11], the iterative adaptive approach (IAA) based on weighted least squares was applied for superresolution. The technique was demonstrated to present higher resolution and finer variance characteristics compared with existing superresolution methods.

In some RAR applications, especially for the surface-to-air case, the target distribution is always sparse. With the prior assumption of sparseness, we firstly introduce the SParse Iterative Covariance-based Estimation (SPICE) algorithm based on the weighted covariance fitting criterion [12] to improve the angular resolution of RAR. To increase the sparseness and location accuracy, a varying penalty on noise term is adopted to extend the SPICE method generally [13]. Compared with the original resolution of RAR system and that of the existing IAA algorithm, the generalized SPICE algorithm can provide higher resolution and location accuracy for sparse target distribution.

In section II, the signal model of RAR azimuth echo is retrospected; in section III and section IV, the SPICE and generalized SPICE approaches are presented; in section V we use simulation results to demonstrate the superior performance of the generalized SPICE algorithm; at last section VI contains our conclusion.

II. Signal model

The two-coordinate RAR locates targets with the range and azimuth estimations. With the development of pulse compression, RAR transmits linear frequency-modulated pulses to obtain high range resolution and signal-to-noise ratio (SNR) gain. Whereas in azimuth, RAR sweeps a narrow beam through the

entire field of view to obtain the angular location. Considering the additive white noise $\mathbf{n} \in \mathbb{C}^{M\times 1}$, this physical process can be modeled as [7]

$$\mathbf{y} = \mathbf{s} \otimes \mathbf{h} + \mathbf{n} \tag{2}$$

where $\mathbf{y} \in \mathbb{C}^{M\times 1}$ is the azimuth echo and "$\otimes$" denotes the convolution operation. $\mathbf{s} \in \mathbb{C}^{K\times 1}$ is the target distribution and $\mathbf{h} \in \mathbb{C}^{L\times 1}$ is the antenna pattern.

Rewriting (2) into the equation set form, we get the spectral analysis model [7]

$$\mathbf{y} = \mathbf{B}\mathbf{s} + \mathbf{n} \tag{3}$$

where $\mathbf{B} = (\mathbf{b}_1, \mathbf{b}_2, \ldots, \mathbf{b}_K)$ is the steering matrix. Usually, we just consider effect of the main lobe of the antenna. Define the antenna vector, the steering matrix $\mathbf{B}$ has the following expression

$$\mathbf{B} = \begin{bmatrix} h_1 & & & \\ h_2 & h_1 & & \\ \vdots & h_2 & \ddots & \\ h_L & \vdots & \ddots & h_1 \\ & h_L & & h_2 \\ & & \ddots & \vdots \\ & & & h_L \end{bmatrix} \tag{4}$$

where $h_l \neq 0,\ l = 1,\ \ldots,\ L$. Correspondingly, there is a determined relationship among M, K and L, namely

$$M = K + L - 1 \tag{5}$$

III. SPICE

Let us assume that the noise covariance matrix

$$E\left(\mathbf{n}\mathbf{n}^H\right) = diag\left(\sigma_1, \sigma_2, \ldots, \sigma_M\right) \tag{6}$$

Then the covariance matrix of $\mathbf{y}$ has the following expression

$$\begin{aligned} \mathbf{R} &= E\left(\mathbf{y}\mathbf{y}^H\right) = \sum_{k=1}^{K} |s_k|^2 \mathbf{a}_k \mathbf{a}_k^H + E\left(\mathbf{n}\mathbf{n}^H\right) \\ &\triangleq \mathbf{A}\mathbf{P}\mathbf{A}^H \end{aligned} \tag{7}$$

where

$$\mathbf{s} \triangleq (s_1, s_2, \ldots, s_K)^T \tag{8}$$

$$\mathbf{A} = [\ \mathbf{B} \quad \mathbf{I}\ ] \triangleq (\mathbf{a}_1, \mathbf{a}_2, \ldots, \mathbf{a}_K) \tag{9}$$

$$\begin{aligned} \mathbf{P} &= diag\left(|s_1|^2, |s_2|^2, \ldots, |s_K|^2, \sigma_1, \sigma_2, \ldots, \sigma_M\right) \\ &\triangleq diag\left(p_1, p_2, \ldots, p_{M+K}\right) \end{aligned} \tag{10}$$

with $\mathbf{I}$ denoting the $M \times M$ identity matrix. To estimate $\mathbf{s}$, define the weighted covariance fitting criterion [12]

$$f = \left\| \mathbf{R}^{-1/2}\left(\mathbf{y}\mathbf{y}^H - \mathbf{R}\right) \right\|^2 \tag{11}$$

where $\|\cdot\|$ denotes the Frobenius norm for matrices, and $\mathbf{R}^{-1/2}$ is the Hermitian positive definite square root of $\mathbf{R}^{-1}$. It was further shown that minimize (11) is equivalent with [12]

$$\min_{\{p_k \geq 0\}} \ \mathbf{y}^H \mathbf{R}^{-1} \mathbf{y} + \|\mathbf{W}\mathbf{p}\|_1 \tag{12}$$

where

$$\mathbf{W} = diag\left(w_1, w_2, \ldots, w_{M+K}\right) \tag{13}$$

$$\mathbf{p} = (p_1, p_2, \ldots, p_{M+K})^T \tag{14}$$

$$w_k = \frac{\|\mathbf{a}_k\|^2}{\|\mathbf{y}\|^2}, k = 1, 2, \ldots M + K \tag{15}$$

The problem presented by (12) is proved to be a semidefinite program which is well known to be convex. Therefore, the classical interior-point polynomial algorithms can be introduced to solve (12). However, the solvers suffer high computationally burden. To solve the problem, the SPICE algorithm firstly convert (12) into another equivalent constrained minimization problem [12]

$$\min_{\{p_k \geq 0\}} \ \mathbf{y}^H \mathbf{R} \mathbf{y} \ \ s.t.\ \|\mathbf{W}\mathbf{p}\|_1 = 1 \tag{16}$$

This can be solved efficiently by iterating the following steps [12]:

$$\rho(i) = \sum_{l=1}^{M+K} w_k^{1/2} p_l(i) \left| \mathbf{a}_k^H \mathbf{R}^{-1}(i)\, \mathbf{y} \right| \tag{17}$$

$$p_k(i+1) = p_k(i) \frac{\left| \mathbf{a}_k^H \mathbf{R}^{-1}(i)\, \mathbf{y} \right|}{w_k^{1/2} \rho(i)}, k = 1, 2, \ldots, K \tag{18}$$

Once p_k was obtained, the target distribution $\mathbf{s}$ can be therefore reconstructed.

Notice that the constraint in (16) is the type of weighted ℓ_1 norm. Therefore, a sparse solution can be obtained by the SPICE algorithm [12]. However, this constraint does not distinguish the signal and noise. Therefore, some of the σ_k may be forced to be zero as a part of the minimization. Because we are interested in finding a sparse solution from the columns of the dictionary $\mathbf{B}$, it make no sense to set some of the noise parameters σ_k to zero. Meanwhile, the sparse estimation of σ_k may lead $\mathbf{R}$ to be not invertible, as (7) shows.

IV. GENERALIZED SPICE

To obtain the sparse and dense estimations of the signal and noise parameters, respectively, we consider the generalized criterion [13]

$$g = \mathbf{y}^H \mathbf{R}^{-1} \mathbf{y} + \|\mathbf{W}_s \mathbf{p}_s\|_1 + \|\mathbf{W}_n \mathbf{p}_n\|_q \tag{19}$$

where

$$\mathbf{p}_s = (p_1, p_2, \ldots, p_K)^T \tag{20}$$

$$\mathbf{p}_n = (p_{K+1}, p_{K+2}, \ldots, p_{M+K})^T \tag{21}$$

$$\mathbf{W}_s = diag\left(w_1, w_2, \ldots, w_M\right) \tag{22}$$

$$\mathbf{W}_n = diag\left(w_{K+1}, w_{K+2}, \ldots, w_{M+K}\right) \tag{23}$$

and $\|\cdot\|_q$ denotes the q-norm, with $q \geq 1$. Thus, the original SPICE is the case where $q = 1$. Define

$$\beta = \mathbf{P}\mathbf{A}^H \mathbf{R}^{-1} \mathbf{y} \triangleq (\beta_1, \beta_2, \ldots, \beta_{M+K})^T \tag{24}$$

the solution to the problem of minimizing (19) can be performed by the following steps iteratively [13]:

$$\lambda = \left(\left\| \mathbf{W}_s^{1/2} \beta_s \right\|_1 + \left\| \mathbf{W}_n^{1/2} \beta_n \right\|_{\frac{2q}{q+1}} \right)^2 \tag{25}$$

$$p_k = \begin{cases} \frac{|\beta_k|}{\sqrt{w_k}\lambda^{1/2}}, k = 1, 2, \ldots, K \\ \frac{|\beta_k|^{\frac{2}{q+1}} \left\| \mathbf{w}_n^{1/2} \beta_n \right\|^{\frac{q-1}{q+1}}_{\frac{2q}{q+1}}}{w_k^{\frac{q}{q+1}} \lambda^{1/2}}, k = K+1, \ldots, M+K \end{cases} \tag{26}$$

where

$$\beta_s = (\beta_1, \beta_2, \ldots, \beta_K)^T \tag{27}$$

$$\beta_n = (\beta_{K+1}, \ldots, \beta_{M+K})^T \tag{28}$$

The initialization of the q-SPICE algorithm can be obtained by [13]

$$p_k = \frac{\mathbf{a}_k^H \mathbf{y}}{\mathbf{a}_k^H \mathbf{a}_k}, k = 1, 2, \ldots, K+M \tag{29}$$

In this work, the q-SPICE algorithm is terminated when the percentage of change between two consecutive iterations falls below a certain level, such as 10^{-4}. Compared with the SPICE algorithm, the q-SPICE algorithm considers the signal and noise terms separately, as shown by (19). Next we will check the performance of the q-SPICE algorithm and discuss the influence of varying norm q.

V. Simulation Results

The ideal $(\sin x/x)^2$ antenna pattern is adopted in our simulation, of which we only consider the main lobe. Certainly, the antennas weighted or applied in practice are also appropriate.

Three point targets are located at $-2.4°$, $-0°$ and $-1.6°$, with normalized amplitudes 0.5, 1 and 1. The circles and the vertical dotted lines that align with these circles represent the true target distribution, and the results of 10 Monte-Carlo trials are shown in each plot. Fig.1(a) shows the antenna pattern with $3°$ main lobe width. Because the three targets are located within the beamwidth, the adjacent targets cannot be distinguished in the real beam echo with SNR = 30dB, as shown in Fig.1(b). Fig.1(c) presents the superresolution result of IAA. We can observe that the IAA algorithm can resolve the three targets successfully. However, the result is not sparse. It is difficult to select the true peaks in the presence of weak peaks provided by the background. The results with varying norms q of the q-SPICE algorithm are shown from Fig.1(d) to Fig.1(g). We can observe that a larger norm brings a stronger robustness and more sparse result when compared with the IAA algorithm. It becomes easier to select the peaks from the estimation of q-SPICE and locate the targets. It can be observed that the amplitude estimation is far away from the truth. However, because the location of the targets has been determined, the least squares (LS) estimator can be introduced to improve the amplitude estimation, as shown in Fig.1(h).

Next we compare the simulation results between the IAA and SPICE methods for the whole scenario matrix. Fig.2(a) shows the typical SAR images. It contains the sparse section indicated by the red square figure, where several boats are available. We use the sparse section for simulations as the truth, as shown in Fig.2(b). Fig.2(c) shows the antenna pattern with 3 degree mainlobe width. Fig.2(d) presents the real beam echo with SNR=25dB, where the adjacent targets cannot be distinguished. Fig.2(e) shows the superresolution result with the IAA method. The targets are resolved but the background

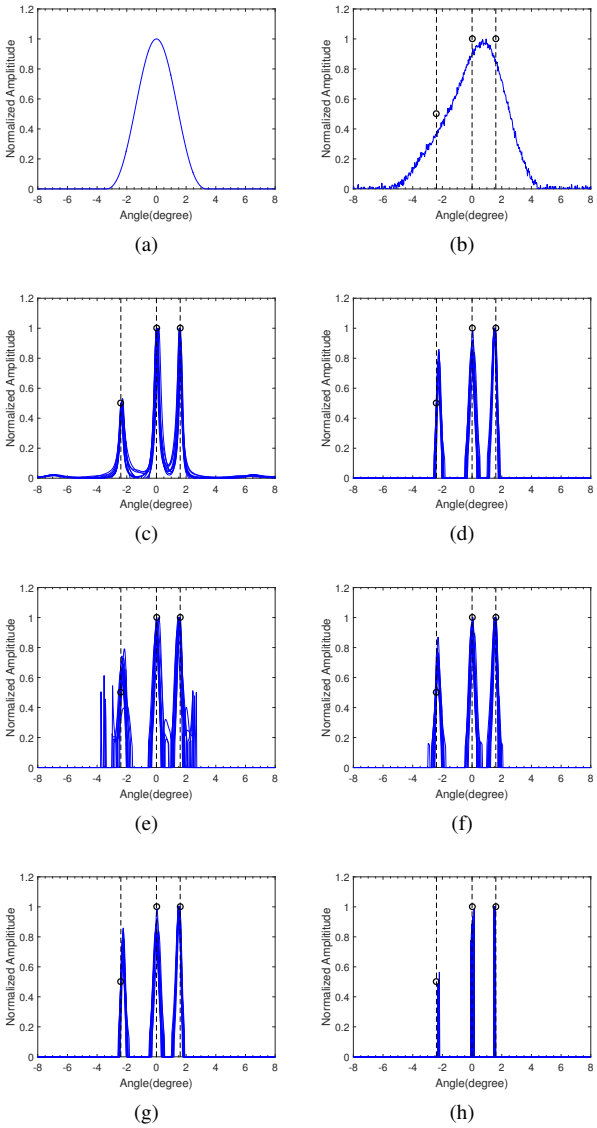

Fig. 1. Simulation results for sparse point targets. (a) Antenna pattern. (b) Real beam echo (SNR=30dB). (c) IAA. (d) q-SPICE (1-norm). (e) q-SPICE (2-norm). (f) q-SPICE (3-norm). (g) q-SPICE (4-norm). (h) q-SPICE with LS (4-norm).

was not suppressed. The results with varying norms of the q-SPICE algorithm are shown from Fig.2(f) to Fig.2(h). We can observe that q-SPICE with 2-norm works worst for background suppression. By contrast, the 4-norm SPICE can suppress the background better.

VI. Conclusion

In this paper, a generalized SPICE algorithm is developed for sparse target location in scanning radar imaging. The method presents different penalties on the signal and noise terms separately. The sparseness of targets are reminisced and a dense noise variance is obtained to decrease estimation error. Compared with the original resolution of RAR system and that of the existing IAA algorithm, the generalized SPICE algorithm can provide higher resolution and location accuracy. However, the generalized SPICE algorithm can not estimate

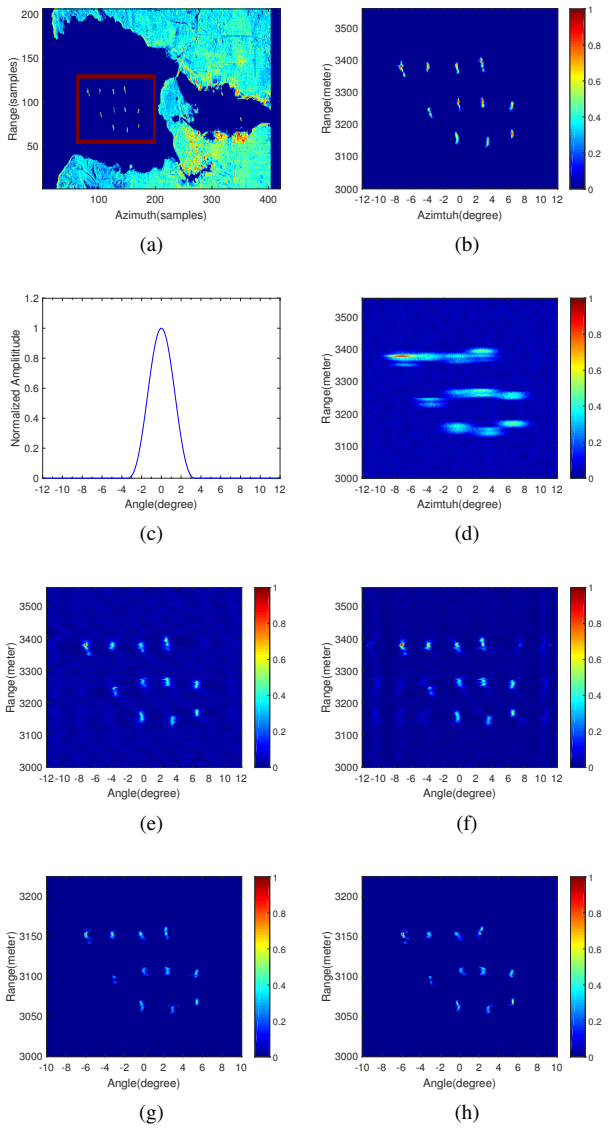

Fig. 2. Simulation results for sparse whole scenario matrix. (a) Typical SAR images. (b) Sparse truth we concentrate on. (c) Antenna pattern. (d) Real beam echo (SNR=25dB). (e) IAA. (f) q-SPICE (2-norm). (g) q-SPICE (3-norm). (h) q-SPICE (4-norm).

the amplitude accurately. Though the amplitude estimation can be improved by LS method, it of great significance to pursue an improved SPICE algorithm to estimate the amplitude more accurately.

REFERENCES

[1] M. I. Skolnik, *Radar Handbook*. The McGraw-Hill Companies, 2008.

[2] A. Gambardella and M. Migliaccio, "On the superresolution of microwave scanning radiometer measurements," *IEEE Geoscience and Remote Sensing Letters*, vol. 5, no. 4, pp. 796–800, Oct 2008.

[3] M. Migliaccio and A. Gambardella, "Microwave radiometer spatial resolution enhancement," *IEEE Transactions on Geoscience and Remote Sensing*, vol. 43, no. 5, pp. 1159–1169, May 2005.

[4] D. Schiavulli, F. Lenti, F. Nunziata, G. Pugliano, and M. Migliaccio, "Landweber method in hilbert and banach spaces to reconstruct the nrcs field from gnss-r measurements," *International Journal of Remote Sensing*, vol. 35, no. 10, pp. 3782–3796, 2014. [Online]. Available: http://dx.doi.org/10.1080/01431161.2014.919676

[5] F. Lenti, F. Nunziata, C. Estatico, and M. Migliaccio, "Spatial resolution enhancement of earth observation products using an acceleration technique for iterative methods," *IEEE Geoscience and Remote Sensing Letters*, vol. 12, no. 2, pp. 269–273, Feb 2015.

[6] J. Guan, J. Yang, Y. Huang, and W. Li, "Maximum a posteriori-based angular superresolution for scanning radar imaging," *IEEE Transactions on Aerospace and Electronic Systems*, vol. 50, no. 3, pp. 2389–2398, July 2014.

[7] Y. Zhang, W. Li, Y. Zhang, Y. Huang, and J. Yang, "A fast iterative adaptive approach for scanning radar angular superresolution," *IEEE Journal of Selected Topics in Applied Earth Observations and Remote Sensing*, vol. 8, no. 11, pp. 5336–5345, Nov 2015.

[8] Y. Zhang, Y. Zhang, Y. Huang, W. Li, and J. Yang, "Angular superresolution for scanning radar with improved regularized iterative adaptive approach," *IEEE Geoscience and Remote Sensing Letters*, vol. 13, no. 6, pp. 846–850, June 2016.

[9] Y. Zhang, Y. Zhang, W. Li, Y. Huang, and J. Yang, "Angular superresolution for real beam radar with iterative adaptive approach," in *2013 IEEE International Geoscience and Remote Sensing Symposium - IGARSS*, July 2013, pp. 3100–3103.

[10] ——, "Divide and conquer: A fast matrix inverse method of iterative adaptive approach for real beam superresolution," in *2014 IEEE Geoscience and Remote Sensing Symposium*, July 2014, pp. 698–701.

[11] Y. Zhang, W. Li, Y. Huang, Y. Zhang, and J. Yang, "Two-channel iterative adaptive approach for scanning radar angular superresolution," in *2016 IEEE Radar Conference (RadarConf)*, May 2016, pp. 1–5.

[12] P. Stoica, P. Babu, and J. Li, "New method of sparse parameter estimation in separable models and its use for spectral analysis of irregularly sampled data," *IEEE Transactions on Signal Processing*, vol. 59, no. 1, pp. 35–47, Jan 2011.

[13] J. Swärd, S. I. Adalbjörnsson, and A. Jakobsson. (2016) Generalized sparse covariance-based estimation. [Online]. Available: https://arxiv.org/abs/1609.03479